processes

MDPI

Article

Expression, Characterization, and Immobilization of a Novel D-Lactate Dehydrogenase from *Salinispirillum* sp. LH 10-3-1

Jianguo Liu *, Xuejiao Jiang, Yaru Zheng, Kaixuan Li, Ruixin Zhang, Jingping Xu, Zhe Wang, Yuxuan Zhang, Haoran Yin and Jing Li *

Department of Biological and Bioenergy Chemical Engineering, College of Chemistry and Chemical Engineering, China University of Petroleum (East China), Qingdao 266580, China; jxj3321@163.com (X.J.); yrzheng0927@163.com (Y.Z.); 17865136839@163.com (K.L.); zrx20031009@163.com (R.Z.); m15621036121@163.com (J.X.); 15829535312@163.com (Z.W.); z17853663898@163.com (Y.Z.); 2203050227@s.upc.edu.cn (H.Y.)

* Correspondence: jianguoliu@upc.edu.cn (J.L.); lijing@upc.edu.cn (J.L.)

Abstract: *Salinispirillum* sp. LH 10-3-1 was newly isolated from the alkali lake water samples collected in Inner Mongolia. In this study, a gene coding for D-lactate dehydrogenase from the strain LH 10-3-1 (*Sa*LDH) was cloned and characterized. The recombinant enzyme was a tetramer with a native molecular mass of 146.2 kDa. The optimal conditions for *Sa*LDH to reduce pyruvate and oxidize D-lactic acid were pH 8.0 and pH 5.0, at 25 °C. Cu^{2+} and Ca^{2+} slightly promoted the oxidation and reduction activities of *Sa*LDH, respectively. To improve the stability of *Sa*LDH, the enzyme was immobilized on $Cu_3(PO_4)_2$-based inorganic hybrid nanoflowers. The results showed that the reduction activity of the hybrid nanoflowers disappeared, and the optimum temperature, specific activity, thermostability, and storage stability of the immobilized *Sa*LDH were significantly improved. In addition, the biotransformation of D-lactic acid to pyruvate catalyzed by *Sa*LDH and the hybrid nanoflowers was investigated. The maximum conversion of D-lactic acid catalyzed by the immobilized *Sa*LDH was 25.7% higher than by free enzymes, and the immobilized *Sa*LDH could maintain 84% of its initial activity after six cycles.

Keywords: D-lactate dehydrogenase; *Salinispirillum* sp.; expression; characterization; immobilization

Citation: Liu, J.; Jiang, X.; Zheng, Y.; Li, K.; Zhang, R.; Xu, J.; Wang, Z.; Zhang, Y.; Yin, H.; Li, J. Expression, Characterization, and Immobilization of a Novel D-Lactate Dehydrogenase from *Salinispirillum* sp. LH 10-3-1. *Processes* **2024**, *12*, 1349. https://doi.org/10.3390/pr12071349

Academic Editor: Hah Young Yoo

Received: 26 April 2024
Revised: 7 June 2024
Accepted: 25 June 2024
Published: 28 June 2024

1. Introduction

D-lactate dehydrogenase (LDH, EC 1.1.1.28) is a key enzyme in the fermentative metabolism of lactic acid bacteria (LAB), which catalyzes the reversible conversion of pyruvate to D-lactic acid with concomitant oxidation of NADH [1]. Nowadays, LDH has become the main enzyme for the production of D-phenyllactic acid (PLA) and optically pure D-lactic acid (LC) [2]. The former (PLA) is a novel and ideal antimicrobial agent in the food industry with a broad spectrum against both bacteria and fungi [3]. The latter (LC) is an important industrial material and has extensive applications in the fields of food, medicine, cosmetics, chemical industry, and environmental protection [4]. In addition, LDH, as an enzyme used for diagnostic biosensors, is also of great significance in identifying the diseases associated with elevated D-lactic acid concentration in urine or serum [5]. So far, LDH has only been found in invertebrates, lower fungi, and prokaryotes, and the catalytic properties of the enzyme for the reduction of pyruvate have been investigated in most reported studies. However, the enzyme characterization for the oxidation of D-lactic acid has been neglected [6]. Furthermore, the low stability of LDH has greatly hampered its industrial application [7].

In order to improve the stability of the enzymes, various immobilization methods including adsorption, encapsulation, cross-linking, and covalent binding have been developed [8,9]. Generally, immobilized enzymes exhibit higher stability than free enzymes [10]. However, in most cases, the enzymatic activities decline after immobilization due to the

changes in enzyme conformation and mass transfer resistance between the substrates and enzymes [11]. In 2012, Ge et al. reported a new method for preparing immobilized enzymes, which not only improved the stability of immobilized enzymes but also enhanced their activity [12]. The immobilized enzymes were called "enzymes inorganic hybrid nanoflowers". Until now, about ten enzymes have been immobilized by this method, and several dual-enzyme and triple-enzyme hybrid nanoflowers have also been reported [13]. However, there has been no report on the immobilization of LDH using the hybrid nanoflowers method, nor has there been any study on the effect of this immobilization method on the performance of the enzyme catalyzing a reversible reaction.

In this study, a novel LDH from the haloalkaliphilic bacterium *Salinispirillum* sp. LH10-3-1 (termed as *Sa*LDH) was cloned and characterized. The recombinant protein was then used as organic component to prepare *Sa*LDH/$Cu_3(PO_4)_2$ hybrid nanoflowers. Further, the reduction and oxidation activities of the immobilized *Sa*LDH on pyruvate and lactate were examined and compared with those of free enzyme. The results show that the immobilized *Sa*LDH exhibited catalytic activity only for the one-way reaction of D-lactic acid to pyruvate, while the free enzyme could catalyze the two-way reaction of this reversible conversion. As far as we know, this phenomenon of enzyme-based hybrid nanoflowers has never been reported. In addition, the optimal temperature, specific activity, thermostability, and storage stability of the immobilized *Sa*LDH have been greatly improved. To the best of our knowledge, this is the first report on the characterization of an LDH from *Salinispirillum* sp.

2. Materials and Methods

2.1. Chemicals and Strains

Sodium pyruvate, NADH, NAD^+, 2-ketobutyric acid, phenylpyruvic acid, benzoic acid, D-lactic acid, L-lactic acid, D-(+)-malic acid, and D-(+)-3-phenyllactic acid were obtained from Shanghai Macklin Biochemical Co., Ltd. (Shanghai, China). Copper phosphate, sodium chloride, potassium chloride, sodium dihydrogen phosphate, zinc chloride, disodium hydrogen phosphate, methanol, ethanol, acetone, and benzene were purchased from Sinopharm Chemical Reagent Corporation (Shanghai, China). All reagents are commercial analytical grade.

Salinispirillum sp. LH10-3-1 (China General Microbiological Culture Collection Center, CGMCC NO: 1.16635 ^{T}) was isolated from alkali lake water samples collected in Inner Mongolia. *Escherichia coli* BL21 (DE3) (Qingke Biology Co., Ltd., Qingdao, China) were used as the host for protein expression.

2.2. Primary and Secondary Structure Analysis

The LDH amino acid sequences sharing high similarities with *Sa*LDH were retrieved from the NCBI database using the BLASTP online service. These sequences were aligned with several functional and verified LDH sequences by the ClustalX2 program. Phylogenetic analysis was performed by the neighbor-joining method using MEGA V11, with one thousand bootstrap replicates. ESPript 3.0 was used to reveal the secondary structure of *Sa*LDH based on the aligned sequences containing LDH from *Leuconostoc mesenteroides* ATCC 8293 (LEUM_1756), with high pyruvate reductase activity, and that of *Pediococcus claussenii* (MH920335), with higher PPA reductase activity [14].

2.3. Gene Cloning

According to the nucleotide sequence encoding *Sa*LDH (NCBI accession number OQ845910), a pair of primers (LDH_F: 5′-GGAATTCATGAAAATCGCCGTCT-3′ and LDH_R: 5′-CCCAAGCTTTTATATCTTAACGACGTGA-3′) were designed to amplify *Sa*LDH gene from the genomic DNA of *Salinispirillum* sp. LH10-3-1 by PCR. The amplified DNA fragment was purified and digested with *Eco*RI and *Hind*III endonucleases (Takara, Dalian, China). Then, the double-digested DNA fragment was ligated into the pET28a(+) plasmid

between the *Eco*RI and *Hind*III sites, and the recombinant plasmid was transformed into *E. coli* BL (DE3) cells for expression.

2.4. Expression and Purification of SaLDH

The recombinant *E. coli* BL21 (DE3) was cultivated in LB medium with kanamycin (50 mg/L) at 37 °C until the absorbance at 600 nm reached 0.8. Then, IPTG was added to 0.5 mM of the culture, and protein expression was induced at 25 °C for 10 h. The cells harvested by centrifugation (8500× *g*, 10 min) were washed and resuspended with Tris-HCl buffer (50 mM, pH 8.0). After cell disruption and centrifugation, the recombinant *Sa*LDH with 6×His-tag in the supernatant was purified by affinity chromatography using a Ni Sephrose 6 Fast Flow column (5 mL, GE Healthcare, Uppsala, Sweden). The detailed process of cell disruption and protein purification was described in our previous works [15]. The purity of the recombinant *Sa*LDH was checked by SDS-PAGE under denaturing conditions.

2.5. Molecular Mass Determination

The molecular mass of the native form of *Sa*LDH was determined by gel filtration as previously described [16]. Briefly, four standard proteins (carbonic anhydrase, glucose oxidase, bovine serum albumin and apoferritin) and *Sa*LDH were applied to a Superdex 200 10/300 GL column (GE Healthcare, Sweden). The molecular mass of native *Sa*LDH was estimated based on the deduced molecular mass curve, which was constructed from the logarithms of the molecular masses of standard proteins versus their elution volumes.

2.6. SaLDH Activity Assay and Protein Quantification

For the reduction activity of *Sa*LDH on pyruvate, the assay mixture (total volume, 1 mL) contained 0.2 mM NADH, 0.6 mM sodium pyruvate, and the relevant amounts of enzyme in Tris-HCl buffer (50 mM, pH 8.0). To measure the oxidation activity of *Sa*LDH on lactate, the reaction mixture (total volume, 1 mL) consisted of 1 mM NAD^+, 50 mM D-lactic acid, and the appropriate enzyme in a citric acid/sodium citrate buffer (50 mM, pH 5.0). Two assays were carried out at 25 °C. The change in absorbance at 340 nm was monitored with a UV–Vis spectrophotometer (UV-2450, SHIMADZU, Kyoto, Japan). One unit of activity was defined as the amount of enzyme that was catalyzing the degradation or formation of 1 μmol NADH per minute under the corresponding reaction conditions. The protein concentration was determined using Bradford's method with bovine serum albumin as the standard [17].

2.7. Characterization of SaLDH

The optimum pH and temperature for the reduction and oxidation activities of *Sa*LDH were assessed at pH 3.0–12.0 and 15–60 °C, respectively. To generate the pH gradient, sodium citrate (50 mM, pH 3.0–6.0), Tris-HCl (50 mM, pH 6.0–9.0) and glycine-NaOH (50 mM, pH 9.0–12.0) buffer solutions were used. The thermal stability of *Sa*LDH was also tested by incubation of the enzyme at different temperatures for 12 h, and the residual activity was measured under the standard conditions.

The effects of the metal ions (Zn^{2+}, Cu^{2+}, Mn^{2+}, Fe^{2+}, Co^{2+}, Ca^{2+}, Mg^{2+}, and Ba^{2+}, final concentration 5 mM), chelating agent EDTA (final concentration 5 mM), organic solvents (DMSO (dimethyl sulfoxide), DMF (N,N-dimethyl formamide), methanol, ethanol, acetone, and benzene, final concentration 5% (v/v)), and NaCl concentration (0–4 M) on *Sa*LDH were determined under the standard activity assay conditions.

To study the substrate specificity of the reduction activity of *Sa*LDH, sodium pyruvate, 2-ketobutyric acid, oxaloacetic acid, sodium phenylpyruvate, α-ketoglutaric acid, benzoic acid, and 3-methyl-2-oxobutyric acid were used as substrates with NADH as a coenzyme. Substrates for the oxidation activity of *Sa*LDH included D-lactic acid, D-(+)-malic acid, and D-(+)-3-phenyllactic acid with NAD^+ as a coenzyme. The kinetic parameters (K_m and V_{max}) for sodium pyruvate, NADH, D-lactic acid, and NAD+ were determined by incubating the enzyme with substrates of various concentrations (0–50 mM) under optimal conditions.

2.8. Synthesis and Characterization of SaLDH/$Cu_3(PO_4)_2$ Hybrid Nanoflowers

To synthesize the *Sa*LDH/$Cu_3(PO_4)_2$ hybrid nanoflowers, 1 mL of copper phosphate aqueous solution (0.1 M) was added into 3 mL of PBS solution (0.2 M, pH 7.4) containing 12 mg *Sa*LDH. After incubation at 4 °C for 36 h, the blue precipitate was collected through centrifugation at 9000× *g* for 10 min. The obtained precipitate was washed thrice with pure water and dried by vacuum freezing.

The morphology, crystal phase, and chemical components of *Sa*LDH/$Cu_3(PO_4)_2$ hybrid nanoflowers were analyzed by Scanning Electron Microscope (SEM, S-4800, HITACHI, Tokyo, Japan), X-ray diffraction (XRD, PANalytical Empyrean, Alemlo, Netherlands), and Fourier Transform Infrared Spectroscopy (FT-IR, Nicolet 6700, Madison, WI, USA), respectively.

2.9. Catalytic Properties of SaLDH/$Cu_3(PO_4)_2$ Hybrid Nanoflowers

The reduction and oxidation activities of the *Sa*LDH/$Cu_3(PO_4)_2$ hybrid nanoflowers were determined using the standard enzyme assay protocol, but the free enzymes (*Sa*LDH) was replaced by the nanoflowers containing the same amount of enzyme.

The optimal catalytic pH and temperature for *Sa*LDH/$Cu_3(PO_4)_2$ hybrid nanoflowers were evaluated at pH 3.0–12.0 and 20–70 °C, respectively. To investigate thermostability, the immobilized enzyme was incubated at 20–80 °C for 12 h, and the residual activities were tested. The storage stability of free, the immobilized *Sa*LDH was assessed at 4 °C for 35 days, and the residual activities were measured weekly.

2.10. Biotransformation of D-Lactic Acid by Free and Immobilized SaLDH

The biotransformation of D-lactic acid (50 mM) and NAD^+ (100 mM) catalyzed by the free *Sa*LDH (0.1 mg/mL) and *Sa*LDH/$Cu_3(PO_4)_2$ hybrid nanoflowers (enzyme content 0.1 mg/mL) was performed under the optimal conditions of a catalyst. D-lactic acid was quantified by UV absorbance as previously described [18].

In addition, the reusability of the *Sa*LDH/$Cu_3(PO_4)_2$ hybrid nanoflowers was also investigated. After the reaction was completed, the immobilized enzyme was recovered by centrifugation at 10,000× *g* for 5 min, and washed with glycine-NaOH (50 mM, pH 8.0) buffer. Then, the washed sample was reused for the next catalytic cycle, and the activity of *Sa*LDH in the first cycle was set as 100%.

3. Results

3.1. Sequence Analysis of SaLDH

The *Sa*LDH gene from *Salinispirillum* sp. LH10-3-1 consists of 993 base pairs and encodes 330 amino acids (NCBI accession No. OQ845910). Alignment analysis of *Sa*LDH with reported LDHs (Figure 1) revealed the substrate binding sites, His-203, Arg-233, Glu-262, His-294, Asp-257 [7], and the conserved GXGXXG (X represents any of the 20 amino acids) motif to bind dinucleotide at positions 151–157 [14].

To reveal the evolutionary status of *Sa*LDH, a phylogenetic tree based on the LDHs of *Salinispirillum* sp. LH10-3-1 and other microorganisms was constructed based on the amino sequences using the neighbor-joining method (Figure 2). The LDH sequences with the highest homology were included in the phylogenetic tree analysis along, with several functional and verified LDH enzymes. The results show that *Sa*LDH falls into a group comprising LDHs which have originated from a marine environment, such as a mangrove forest (*Hahella* sp. CCB-MM4 [19], *Mangrovitalea sediminis* [20]), sea urchin (*Colwellia echini*) [21], and intertidal sediment (*Marinobacter antarcticus*) [22]. *Sa*LDH were classified into a small clade with the LDHs of *Natronospirillum operosum* sp., which shares the highest identity of 75.45%.

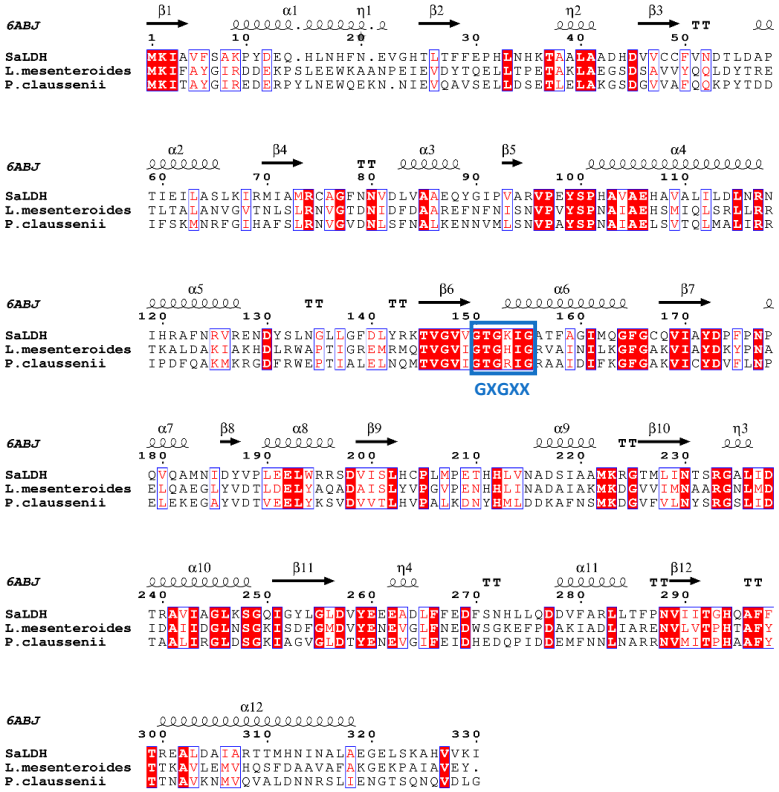

Figure 1. Alignment of *Sa*LDH from *Salinispirillum* sp. LH10-3-1 with LDH of *L. mesenteriodes* and *P. claussennii* based on the amino acid sequences. The LDH from *Pseudomonas aeruginosa* (PDB ID 6AJB) is used as top secondary structure. The nucleotide-binding signature domain GXGXXG is marked with blue square.

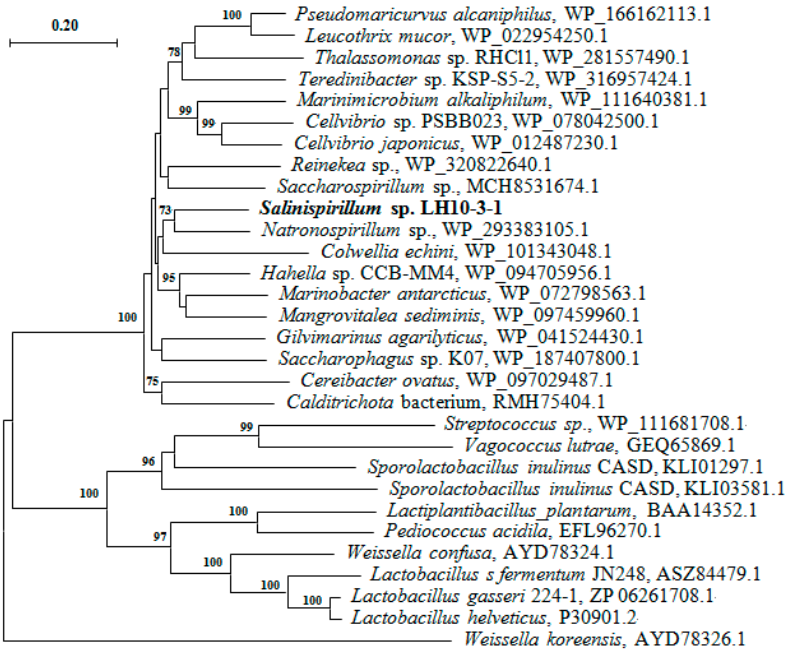

Figure 2. Phylogenetic tree of *Sa*LDH, D-lactate dehydrogenases of the most related relatives and functional verified microorganisms based on their amino acid sequences. The phylogenetic tree was constructed using the neighbor-joining method with 1000 bootstrap replicates (using MEGA 11.0 software).

3.2. Enzyme Purification and Molecular Mass Determination

The total reduction activity and oxidation activity from the initial crude extract were 4603.7 U and 3161.4 U, respectively. After the affinity chromatography step, the specific reduction activity and oxidation activity of the purified *Sa*LDH were 107.5 U/mg and 40.9 U/mg, respectively, with activity yields of 36.1% and 20.0% (Table 1).

Table 1. Comparison of *Sa*LDH specific enzyme activity and yield.

Sample	Specific Activity (U/mg)		Yield (%)	
	Reduction Activity	Oxidation Activity	Reduction Activity	Oxidation Activity
Initial crude extract	8.0	5.5	100.0	100.0
Purified *Sa*LDH	107.5	40.9	36.1 [a]	20.0
Immobilized *Sa*LDH	0	66.3	0	162.1 [b]

[a] The yield = (total reduction activity in initial crude extract/ total reduction activity of purified *Sa*LDH) × 100%.
[b] The yield = (specific activity of immobilized *Sa*LDH/specific activity of purified *Sa*LDH) × 100%.

SDS-PAGE analysis of the purified *Sa*LDH (Figure 3a) showed a single major band near 37 kDa, which was close to the theoretical value of the enzyme (36.3 kDa). The native molecular mass of *Sa*LDH was determined to be approximately 146.2 kDa on the Superdex 200 10/300 GL column (Figure 3b). Thus, the recombinant *Sa*LDH should be a tetramer.

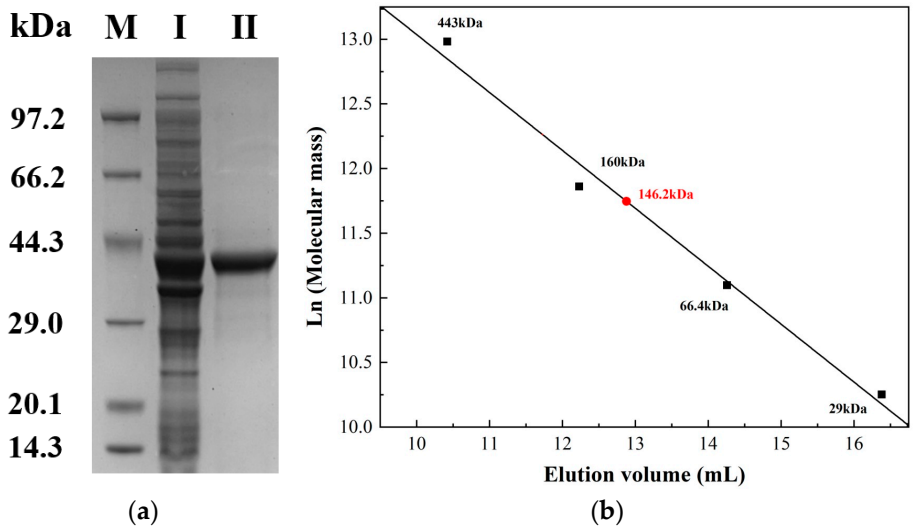

Figure 3. (**a**) SDS-PAGE analysis of *Sa*LDH samples under reducing condition. M, protein marker; I, crude enzyme solution from induced cells; II, purified recombinant *Sa*LDH. (**b**) Molecular mass estimation of the native *Sa*LDH based on the gel filtration analysis using a Superdex 200 10/300 GL column. Four standard proteins were apoferritin (443 kDa), glucose oxidase (160 kDa), bovine serum albumin (66.4 kDa), and carbonic anhydrase (29 kDa).

3.3. Effects of pH and Temperature on SaLDH Activity

The optimal pH values for the reduction and oxidation activity of *Sa*LDH were pH 8.0 and pH 5.0 (Figure 4a), respectively, and the optimal temperature was 25 °C (Figure 4b). In addition, except for the optimal temperature, the relative reduction activity of *Sa*LDH was always higher than its relative oxidation activity, especially in the temperature range of 35 °C to 60 °C. Figure 4c illustrated the thermostability of *Sa*LDH. It can be seen that the thermostability of the enzyme was not ideal, and it would quickly deactivate when the temperature exceeded 35 °C.

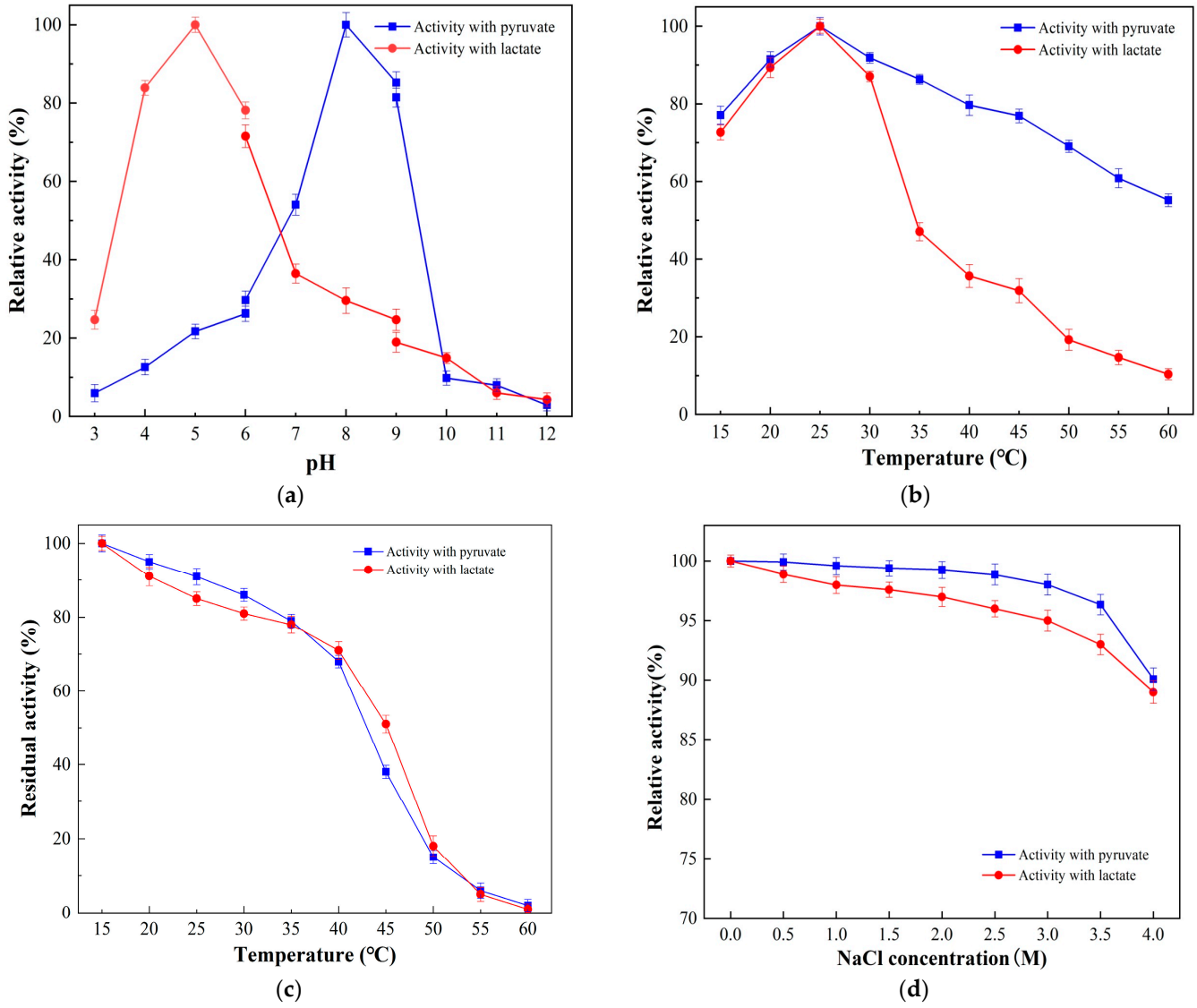

Figure 4. Enzymatic properties of recombinant *Sa*LDH. (**a**) Effect of pH on reduction and oxidation activity. (**b**) Effect of temperature on reduction and oxidation activity. Activity was measured at 15–60 °C for 15 min. (**c**) Thermostability of *Sa*LDH. (**d**) Effect of NaCl concentration on reduction and oxidation activity.

3.4. Effects of Metal Ions, Organic Solvents, and NaCl Concentration on SaLDH Activity

The effects of metal ions and organic solvents on the activity of *Sa*LDH were also investigated. As shown in Table 2, Cu^{2+} slightly stimulated the oxidation activity of *Sa*LDH, but strongly inhibited the reduction activity of the enzyme. On the contrary, Ca^{2+} had a promoting effect on the reduction activity of *Sa*LDH but led to a loss of 68.3% in the enzyme's oxidation activity. In addition, Co^{2+} had little effect on both the reduction and oxidation activities of *Sa*LDH, while the other metal ions had mild or moderate inhibitory effects on enzyme activity. The presence of EDTA did not significantly affect the activity of *Sa*LDH, indicating that the enzyme was not metal-dependent. In the organic solvents studied (Table 2), DMSO, DMF, methanol, ethanol, and acetone had no effect on the activity of *Sa*LDH, while the inhibitory effect of benzene on *Sa*LDH activity was about 10%.

Table 2. Effect of metal ions, EDTA, and organic solvents on *Sa*LDH activity.

Additive	Relative Activity (%)	
	Activity with Pyruvate	Activity with Lactate
Control	100.0 ± 0.0	100.0 ± 0.0
Zn^{2+}	86.3 ± 1.6	78.9 ± 1.5
Cu^{2+}	24.2 ± 0.4	107.9 ± 0.6
Mn^{2+}	52.5 ± 0.3	64.4 ± 0.9
Co^{2+}	102.3 ± 1.2	101.2 ± 0.3
Ca^{2+}	105.8 ± 0.5	31.7 ± 0.4
Mg^{2+}	63.9 ± 1.1	65.3 ± 1.8
Ba^{2+}	61.6 ± 0.5	71.9 ± 0.6
Fe^{3+}	73.0 ± 0.9	73.6 ± 1.3
EDTA	96.5 ± 1.2	95.3 ± 1.4
DMSO	99.9 ± 2.1	98.9 ± 1.9
DMF	99.9 ± 1.8	99.0 ± 2.1
Methanol	99.7 ± 2.5	98.6 ± 1.8
Ethanol	99.3 ± 1.4	97.3 ± 1.7
Acetone	98.8 ± 1.7	97.1 ± 2.1
Benzene	90.8 ± 2.2	91.2 ± 1.9

Figure 4d shows the influence of NaCl concentration on *Sa*LDH activity. It can be seen that the enzyme had excellent salt resistance and could still maintain nearly 90% enzyme activity at a NaCl concentration of 4.0 M. Another result obtained from Figure 4d is that the relative reduction activity of *Sa*LDH was higher than its relative oxidation activity within the NaCl concentration range of 0.5–4.0 M.

3.5. Substrate Specificity and Kinetic Parameters of SaLDH

The substrate specificity of *Sa*LDH was examined using various potential substrates. As shown in Table 3, *Sa*LDH had reduction activity toward sodium pyruvate (relative activity, 100%), 2-ketobutyric acid (97.9%), α-ketoglutaric acid (79.8%), benzoic acid (69.2%), oxaloacetic acid (74.2%), and phenylpyruvic acid (30.3%). As for the oxidation activity, D-lactic acid (100%), D-(+)-malic acid (88.4%), and D-(+)-3-phenyllactic acid (84.6%) were substrates of *Sa*LDH, but L-lactic acid was inert.

Table 3. Substrate specificity of *Sa*LDH.

Substrates	Relative Activity (%)	Specific Activity (U/mg)
Sodium pyruvate	100.0	107.5
2-Ketobutyric acid	97.9	105.2
Oxaloacetic acid	74.2	79.8
Phenylpyruvic acid	30.3	32.6
α-Ketoglutaric acid	79.8	85.8
Benzoic acid	69.2	74.4
D-lactic acid	100.0	40.9
L-lactic acid	0.0	0.0
D-(+)-Malic acid	88.4	36.2
D-(+)-3-Phenyllactic acid	84.6	34.6

The kinetic parameters of *Sa*LDH were determined using sodium pyruvate, NADH, D-lactic acid, and NAD+ as substrates (Table 4). It can be found that the K_m values of the above four substrates were estimated to be 0.34, 0.52, 1.71, and 0.46 mM, respectively. Therefore, *Sa*LDH had the highest affinity for sodium pyruvate. In addition, the V_{max} of the four substrates were determined to be 561.7, 240.5, 197.2, and 383.6 U/mg, respectively.

Table 4. The apparent Km values of LDHs from different microorganisms to pyruvate, NADH, D-lactic acid and NAD^+.

Strains	K_m (mM)				References
	Pyruvate	NADH	D-Lactic Acid	NAD^+	
Salinispirillum sp. LH 10-3-1	0.34	0.52	1.71	0.46	This work
Bacillus coagulans	5.9	n.d.	5.94	n.d.	[1]
Leuconostoc mesenteroides	0.09	0.05	n.d.	n.d.	[23]
Lacobacillus bulgaricus	1.6	n.d.	133	n.d.	[24]
L. plantarum	1.2	n.d.	7.0	n.d.	[25]
L. helveticus CNRZ 32	0.64	n.d.	68	n.d.	[26]
Staphylococcus sp. LDH-1	0.67	n.d.	8.5	n.d.	[27]

Note: n.d., not determined.

3.6. Synthesis and Characterization of SaLDH/$Cu_3(PO_4)_2$ Hybrid Nanoflowers

The *Sa*LDH/$Cu_3(PO_4)_2$ hybrid nanoflowers were synthesized from 3.0 mg/mL *Sa*LDH and 25 mM copper phosphate. The immobilization yields of this immobilization method based on enzyme weight and specific enzyme activity were 73.9% and 162.1%, respectively. After vacuum freeze-drying, the resulting *Sa*LDH/$Cu_3(PO_4)_2$ hybrid nanoflowers appeared as a blue powder. The morphology of the nanoflowers was determined by SEM. In the low-resolution SEM image shown in Figure 5a, the nanoflowers were spherical, with uniform structure and good monodispersity. However, the high-resolution SEM image (Figure 5b) exhibited a layered flower pattern. In addition, it can also be seen from Figure 4a that the diameter of most nanoflowers was about 5 μm.

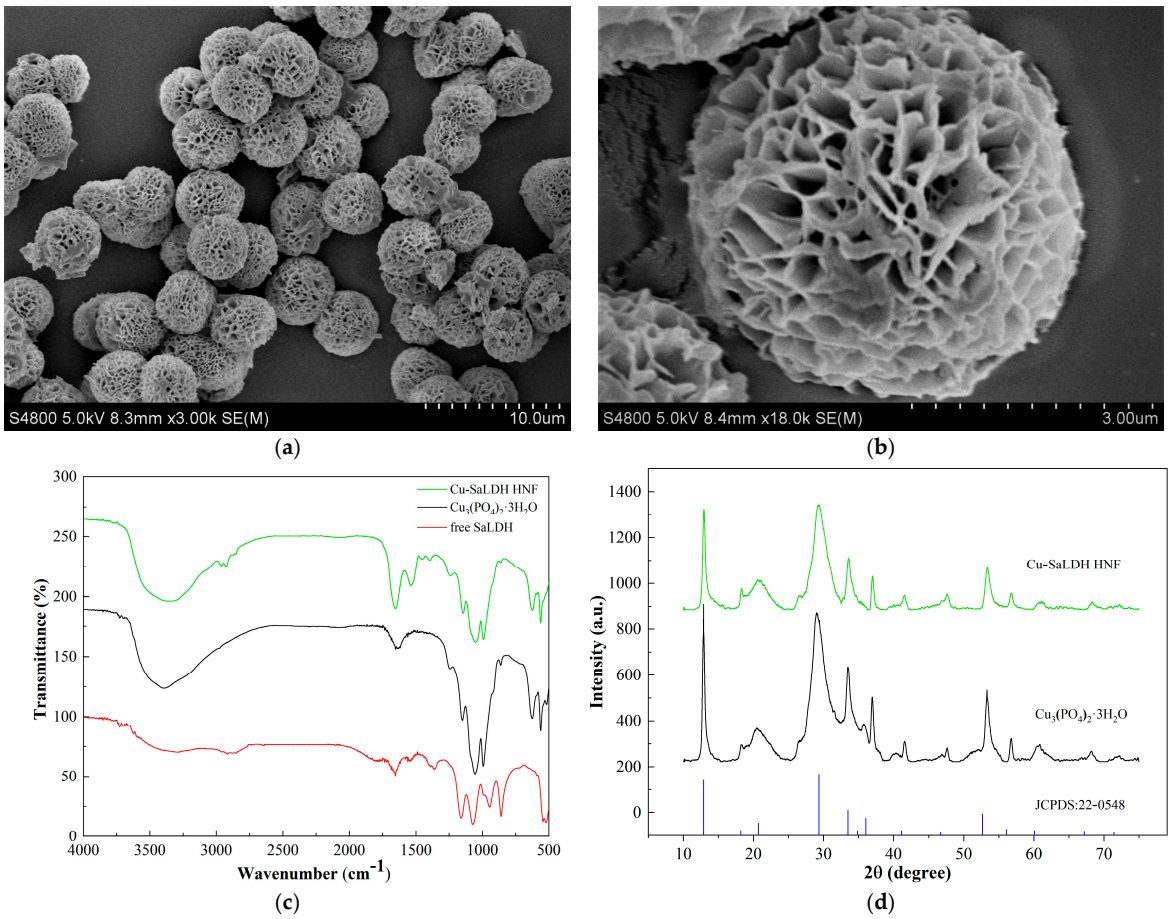

Figure 5. SEM images (**a**,**b**) of *Sa*LDH/$Cu_3(PO_4)_2$ hybrid nanoflowers (Cu-*Sa*LDH HNF). FT-IR spectra (**c**) and XRD patterns (**d**) of free *Sa*LDH, $Cu_3(PO_4)_2$ particles, and Cu-*Sa*LDH HNF.

To investigate the composition of *Sa*LDH/$Cu_3(PO_4)_2$ hybrid nanoflowers, FT-IR analysis was performed. The FT-IR spectra of *Sa*LDH, $Cu_3(PO_4)_2$ particles, and *Sa*LDH/$Cu_3(PO_4)_2$ hybrid nanoflowers were shown in Figure 5c. As can be seen, the nanoflowers contained the main characteristic absorption peaks of *Sa*LDH and $Cu_3(PO_4)_2$ particles, and no new absorption peak and obvious peak shift were found. Therefore, *Sa*LDH was immobilized on the nanoflowers by self-assembly instead of covalent bonds [12,28]. Additionally, the absorption peaks of the main functional groups in the FT-IR spectrum are listed in Supplementary Table S1.

Figure 5d illustrates the XRD patterns of the $Cu_3(PO_4)_2{\cdot}3H_2O$ and *Sa*LDH/$Cu_3(PO_4)_2$ hybrid nanoflowers. It can be found that all diffraction peaks of the nanoflowers were same as those of $Cu_3(PO_4)_2{\cdot}3H_2O$, and the peaks presented in both curves can be indexed to the JCPDS card no. 22-0548. These results indicate that the *Sa*LDH/$Cu_3(PO_4)_2$ hybrid nanoflowers were well crystallized and the inorganic composition of the nanoflowers was copper phosphate trihydrate [29].

3.7. Catalytic Properties of SaLDH/$Cu_3(PO_4)_2$ Hybrid Nanoflowers

Before characterizing the properties of the *Sa*LDH/$Cu_3(PO_4)_2$ hybrid nanoflowers, their catalytic activities for the reversible reaction between pyruvate and D-lactic acid were first studied using a standard enzyme assay. The results showed that the immobilized enzyme exhibited catalytic activity only for the one-way reaction of D-lactic acid to pyruvate. Therefore, the oxidation activity of the nanoflowers was subsequently examined.

Figure 6a,b showed the effects of pH and temperature on the oxidation activity of *Sa*LDH/$Cu_3(PO_4)_2$ hybrid nanoflowers. It can be seen that the optimum reaction conditions of the immobilized enzyme were pH 8.0 and 50 °C. Under these optimal conditions, the specific activity of the nanoflowers reached 66.3 U/mg (Table 1), which was 1.62 times that of *Sa*LDH (40.9 U/mg). In addition, the nanoflowers maintained over 80% of their maximum oxidation activity between pH 6.0 and 9.0 and from 40 to 55 °C, respectively. Furthermore, the immobilized enzyme exhibited much higher thermostability than free *Sa*LDH (Figure 6c), especially in the temperature range of 40–65 °C. For example, after incubation at 60 °C for 12 h, the nanoflowers retained 72.3% of their initial activity, while the residual activity of free *Sa*LDH was only 9.8%.

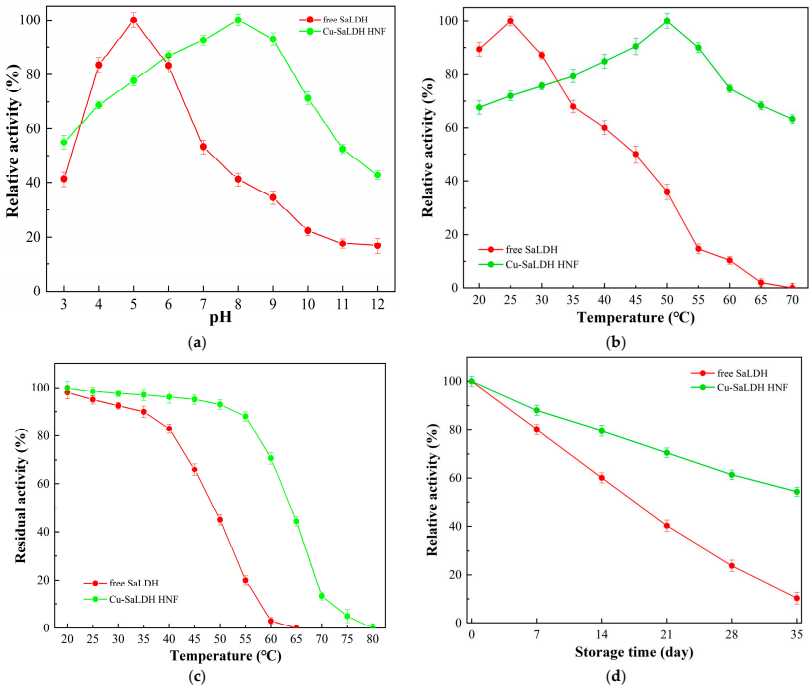

Figure 6. Effects of pH (**a**) and temperature (**b**) on enzyme activity of the free *Sa*LDH and Cu-SaLDH HNF. Thermostability (**c**) and storage stability (**d**) of the free *Sa*LDH and Cu-*Sa*LDH HNF.

The storage stability of the free and immobilized *Sa*LDH was determined at 4 °C for 35 days and the results are shown in Figure 6d. As can be seen, the activity profile of the free *Sa*LDH decreased much faster than that of immobilized enzyme. After 35 days of storage at 4 °C, the free *Sa*LDH lost nearly 90% of its initial activity, while the nanoflowers only lost 47% of their initial activity.

3.8. Biotransformation of D-Lactic Acid by Free and Immobilized SaLDH

The biotransformation of D-lactic acid to pyruvate catalyzed by the free *Sa*LDH (pH 5.0, 25 °C, enzyme content: 0.1 mg/mL) and *Sa*LDH/$Cu_3(PO_4)_2$ hybrid nanoflowers (pH 8.0, 50 °C, enzyme content: 0.1 mg/mL) was performed. As shown in Figure 7a, the maximum conversion of D-lactic acid catalyzed by the free and immobilized *Sa*LDH was 59.6% and 85.3%, respectively. As for the reusability of the nanoflowers (Figure 7b), it was found that the immobilized enzyme could maintain 93%, 86%, and 78% of its initial activity after 4, 6, and 8 cycles, respectively.

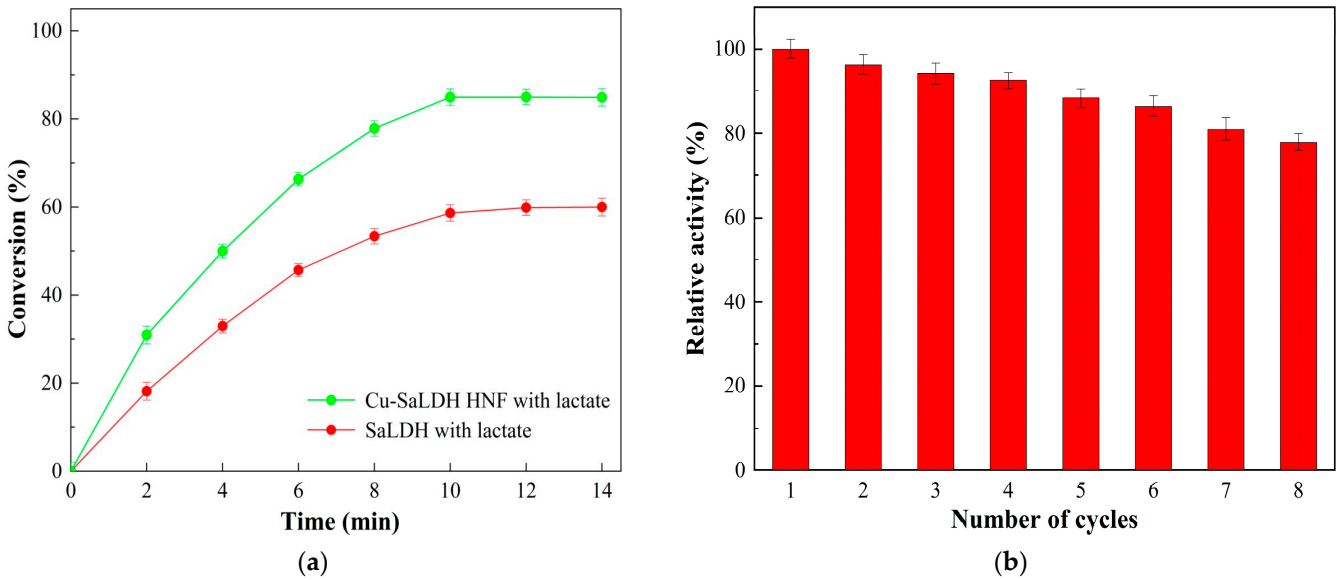

Figure 7. (**a**) Time course of the biotransformation of D-lactic acid to pyruvate catalyzed by the free *Sa*LDH and Cu-*Sa*LDH HNF. Reaction conditions for using free *Sa*LDH: pH 5.0, 25 °C, enzyme content: 0.1 mg/mL; Reaction conditions for using Cu-*Sa*LDH HNF: pH 8.0, 50 °C, enzyme content: 0.1 mg/mL. (**b**) Reusability of Cu-*Sa*LDH HNF for catalyzing the biotransformation of D-lactic acid to pyruvate.

4. Discussion

LDH is not only a critical enzyme in the fermentation metabolism of LAB [1,30], but also an important industrial enzyme that can be used for medical diagnosis [5], and the production of PLA and optically pure LC [3,31]. Presently, most of the reported LDHs are found in LAB strains [32], but due to their low stability, it is necessary to search for new sources [7,33]. In this work, a novel LDH from a haloalkaliphilic bacterium *Salinispirillum* sp. LH10-3-1 (*Sa*LDH) was cloned, characterized, and immobilized. To our knowledge, this is the first report on the characterization of an LDH from *Salinispirillum* sp.

Alignment analysis of the *Sa*LDH with reported LDHs indicated that His-203, Arg-233, Glu-262, His-294, and Asp-257 are essential residues for substrate binding and catalytic activity of LDH [20,34]. Their location in the active site of the enzyme has been confirmed by the crystal structure of the LDH from *L. helveticus* [35]. The pairwise distance analysis indicated that the similarity between *Sa*LDH and the other LDHs ranged from 29% to 75%, and the highest identity LDH with *Sa*LDH came from *N. operosum*, which was a haloalkaliphilic bacterium isolated from cyanobacterium biomass. The topological structure of the phylogenetic tree indicated that *Sa*LDH was clustered with LDHs that originated

from marine habitats. This marine LDH group is located quite distinctly from the LDHs described in the previous publications, including those from lactic acid bacteria, which implies that it could possess unique property traits. At this point, no investigation had been performed regarding the LDH proteins of this marine cluster, therefore research on the enzymatic characteristics of *Sa*LDH might shed some light on the enzymatic property preferences for LDH proteins of this marine cluster.

After molecular mass determination, *Sa*LDH was found to be a tetramer with a molecular mass of 146.2 kDa (gel filtration chromatography) or 37 kDa (SDS-PAGE). The tetrameric structure of LDH is rarely reported, because LDHs mostly exist in the form of homodimers with subunit molecular mass of 32–40 kDa [7,32]. In addition, a dimeric LDH with subunit molecular mass of 48 kDa (beyond the above range) was also found in *Sulfolobus tokodaii* strain 7 [36].

The optimal pH value for the reduction activity of LDH varies greatly in the literature, ranging from 4.0 to 8.6 [26]. In this work, *Sa*LDH exhibited the highest reduction activity at pH 8.0, within the aforementioned pH range. However, the optimum pH for the oxidation activity of *Sa*LDH (pH 5.0) is the lowest among the known LDHs (optimal pH: 7.8–9.6) [37]. In addition, the optimal temperature of *Sa*LDH (25 °C) was the same as that of LDH from *L. murinum* [27], and this value is the smallest among the reported LDHs [37]. Regarding the thermostability of LDH, it is difficult to compare the literature data due to different testing methods. *Sa*LDH was only stable below 35 °C, but its thermostability could be improved through gene mutation [38] or immobilization [23].

As for the effect of metal ions on the reduction activity of LDH, it was reported that Mg^{2+} and Mn^{2+} were activators while Ca^{2+} was an inhibitor for the enzyme of *Lactobacillus* sp. ZX1 [28]. On the contrary, Ca^{2+} slightly stimulated *Sa*LDH activity, while Mg^{2+} and Mn^{2+} moderately inhibited enzyme activity. A similar phenomenon was also observed in the oxidative activity of LDH. For example, Cu^{2+} was found to be a strong inhibitor for the enzyme of *S. tokodaii* strain 7 [36], while Cu^{2+} had a slight promoting effect on the oxidation activity of *Sa*LDH. These results indicated that the structures of LDHs from different sources might be different under the stimulation of the same metal ions [39].

The influences of organic solvents and NaCl concentration on LDH activity have rarely been reported in the literature. In this study, it was found that DMSO, DMF, methanol, ethanol, and acetone did not affect both reduction and oxidation activities of *Sa*LDH. In addition, even at a NaCl concentration of 4.0 M, the enzyme could maintain nearly 90% of its original activity. The salt tolerance of *Sa*LDH may be related to the fact that *Salinispirillum* sp. LH10-3-1 is a haloalkaliphilic bacterium [16]. The excellent organic solvent and salt resistance of *Sa*LDH will be beneficial for its application in partially hydrophobic and high salt environments.

In the previous literature, LDH has been reported to have broad substrate specificity [24,32]. This property is shared by *Sa*LDH of *Salinispirillum* sp. LH10-3-1 (See Table 3). In addition, the apparent K_m value of *Sa*LDH for pyruvate (or D-lactic acid, Table 4) was lower than those from *B. coagulans* [1], *L. bulgaricus* [24], *L. plantarum* [40], *L. helveticus* CNRZ 32 [26], and *Staphylococcus* sp. LDH-1 [27]. Therefore, *Sa*LDH possesses better substrate affinity than the aforementioned LDHs.

Considering that the thermostability of *Sa*LDH is not ideal (only stable below 35 °C), the enzyme was immobilized using the hybrid nanoflowers method [28]. The analysis results of SEM, FT-IR, and XRD (Figure 5) confirmed the successful synthesis of *Sa*LDH/$Cu_3(PO_4)_2$ hybrid nanoflowers [41]. The reason for choosing copper phosphate is that Cu^{2+} not only promotes the oxidation activity of *Sa*LDH, but also strongly inhibits its reduction activity. We expected that through the immobilization process, *Sa*LDH would become the catalyst for an irreversible reaction thus improving the conversion rate of the substrate. The results showed that the reduction activity of immobilized *Sa*LDH completely disappeared as expected. This phenomenon of enzyme-based hybrid nanoflowers has never been reported before. In order to make sure the immobilized *Sa*LDH only have reduc-

tion activity, the *Sa*LDH/$Ca_3(PO_4)_2$ hybrid nanoflowers are currently being synthesized based on the effect of Ca^{2+} on enzyme activity.

In addition, the comparison of catalytic properties between the free *Sa*LDH and hybrid nanoflowers showed that the optimum temperature and specific activity of immobilized *Sa*LDH increased by 25 °C (Figure 6b) and 62%, respectively. Furthermore, the thermostability (Figure 6c) of hybrid nanoflowers was also significantly improved. Similar improvements in enzymatic properties were observed in the hybrid nanoflowers composed of other enzymes such as laccase [29] and urease [42], which may be due to the enhanced stiffness and conformational flexibility of enzyme-based hybrid nanoflowers to prevent conformational changes at high temperatures [11]. Furthermore, the enhanced activity of *Sa*LDH in nanoflowers may be attributed to the high surface area of the nanoflower, high optimal temperature, and the interactions between *Sa*LDH and the nanoscale microenvironment containing Cu^{2+} ions [29].

Since the immobilized *Sa*LDH only had oxidation activity, this study investigated the biotransformation of D-lactic acid to pyruvate catalyzed by the free *Sa*LDH and *Sa*LDH/$Cu_3(PO_4)_2$ hybrid nanoflowers. The results showed that the maximum conversion of D-lactic acid catalyzed by the immobilized *Sa*LDH was 25.7% higher than by the free enzyme (Figure 7a). In addition, the immobilized *Sa*LDH could maintain 84% of its initial activity after six cycles (Figure 7b), indicating that the hybrid nanoflowers had good operational stability.

In summary, this work provides a novel D-lactate dehydrogenase from *Salinispirillum* sp. LH10-3-1. After systematic characterization and comparison of the reducing and oxidizing activities of *Sa*LDH, the enzyme was immobilized on the $Cu_3(PO_4)_2$-based inorganic hybrid nanoflowers. With the disappearance of reducing activity, the specific activity, optimal temperature, thermostability, storage stability and operational stability of the oxidation activity of the immobilized *Sa*LDH was significantly improved. These results will expand people's understanding of the enzyme and provide new ideas for the selection of metal ions in the synthesis of organic–inorganic nanoflowers. In addition, these outstanding characteristics make immobilized *Sa*LDH a promising biocatalyst for industrial application.

Supplementary Materials: The following supporting information can be downloaded at: https://www.mdpi.com/article/10.3390/pr12071349/s1, Table S1. The Correspondence between functional groups and absorption peaks in the FT-IR spectra.

Author Contributions: Conceptualization, J.L. (Jianguo Liu) and X.J.; methodology, J.L. (Jianguo Liu), X.J. and Y.Z. (Yaru Zheng); validation, K.L. and R.Z.; formal analysis, J.X.; investigation, Z.W.; resources, J.L. (Jing Li); data curation, Y.Z. (Yuxuan Zhang); writing—original draft preparation, J.L. (Jianguo Liu); writing—review and editing, J.L. (Jing Li); visualization, H.Y.; supervision, J.L. (Jing Li); project administration, J.L. (Jianguo Liu); funding acquisition, J.L. (Jianguo Liu). All authors have read and agreed to the published version of the manuscript.

Funding: This work was supported by the National Natural Science Foundation of China (No. 21473256 and 21776310), the Key Research and Development Project of Shandong Province (No. 2019GSF107077), and Key Technology of Independent Innovation of Qingdao West Coast New Economic District (2020-6).

Data Availability Statement: The research data of this article can be obtained from the corresponding author J.L. (Jianguo Liu) and J.L. (Jing Li) through reasonable requests.

Conflicts of Interest: The authors declare no conflicts of interest.

References

1. Wang, L.; Cai, Y.; Zhu, L.; Guo, H.; Yu, B. Major role of NAD-dependent lactate dehydrogenases in the production of L-lactic acid with high optical purifity by the thermophile *Bacillus coagulans*. *Appl. Environ. Microb.* **2014**, *80*, 7134–7141. [CrossRef] [PubMed]
2. Gu, S.A.; Jun, C.; Joo, J.C.; Kim, S.; Lee, S.H.; Kim, Y.H. Higher thermostability of L-lactate dehydrogenases is a key factor in decreasing the optical purity of D-lactic acid produced from *Lactobacillus coryniformis*. *Enzym. Microb. Tech.* **2014**, *58–59*, 29–35. [CrossRef] [PubMed]

3. Mu, W.; Yu, S.; Jiang, B.; Li, X. Characterization of D-lactate dehydrogenase from *Pediococcus acidilactici* that converts phenylpyruvic acid into phenyllactic acid. *Biotechnol. Lett.* **2012**, *34*, 907–911. [CrossRef] [PubMed]
4. Kuo, Y.C.; Yuan, S.F.; Wang, C.A.; Huang, Y.J.; Guo, G.L.; Hwang, W.S. Production of optically pure L-lactic acid from lignocellulosic hydrolysate by using a newly isolated and D-lactate dehydrogenase gene-deficient *Lactobacillus paracasei* strain. *Bioresour. Technol.* **2015**, *198*, 651–657. [CrossRef] [PubMed]
5. Leonida, M.D.; Starczynowski, D.T.; Waldman, R.; Aurian-Blajeni, B. Polymeric FAD used as enzyme-friendly mediator in lactate detection. *Anal. Bioanal. Chem.* **2003**, *376*, 832–837. [CrossRef] [PubMed]
6. Richter, N.; Zienert, A.; Hummel, W. A single-point mutation enables lactate dehydrogenase from *Bacillus* subtilis to utilize NAD^+ and $NADP^+$ as cofactor. *Eng. Life Sci.* **2011**, *11*, 26–36. [CrossRef]
7. Jun, C.; Sa, Y.S.; Gu, S.A.; Joo, J.C.; Kim, S.; Kim, K.J.; Kim, Y.H. Discovery and characterization of a thermostable D-lactate dehydrogenase from *Lactobacillus jensenii* through genome mining. *Process Biochem.* **2013**, *48*, 109–117.
8. Zhou, W.; Zhang, W.; Cai, Y. Enzyme-enhanced adsorption of laccase immobilized graphene oxide for micro-pollutant removal. *Sep. Purif. Technol.* **2022**, *294*, 121178. [CrossRef]
9. Singh, T.A.; Jajoo, A.; Bhasin, S. Optimization of various encapsulation systems for efficient immobilization of actinobacterial glucose isomerase. *Biocatal. Agric. Biotechnol.* **2020**, *29*, 101766. [CrossRef]
10. Ansari, S.A.; Husain, Q. Potential applications of enzymes immobilized on/in nano materials: A review. *Biotechnol. Adv.* **2012**, *30*, 512–523. [CrossRef]
11. Duan, L.; Li, H.; Zhang, Y. Synthesis of hydrid nanoflower-based carbonic anhydrase for enhanced bioactivity and stability. *ACS Omega* **2018**, *3*, 18234–18241. [CrossRef]
12. Ge, J.; Lei, J.; Zare, R.N. Protein–inorganic hybrid nanoflowers. *Nat. Nanotechnol.* **2012**, *7*, 428–432. [CrossRef]
13. Aydemir, D.; Gecili, F.; Özdemir, N.; Ulusu, N.N. Synthesis and characterization of a triple enzyme-inorganic hybrid na noflower (TrpE@ihNF) as a combination of three pancreatic digestive enzymes amylase, protease and lipase. *J. Biosci. Bioeng.* **2020**, *129*, 679–686. [CrossRef]
14. Cheng, Y.Y.; Park, T.H.; Seong, H.; Kim, T.J.; Han, N.S. Biological characterization of D-lactate dehydrogenase responsible for high-yield production of D-phenyllactic acid in *Sporolactobacillus inulinus*. *Microb. Biotechnol.* **2022**, *15*, 2717–2729. [CrossRef]
15. Liu, D.; Xi, L.; Han, D.; Dou, K.; Su, S.; Liu, J. Cloning, expression, and characterization of a novel nitrilase, PaCNit, from *Pannonibacter carbonis* Q4.6. *Biotechnol. Lett.* **2019**, *41*, 583–589. [CrossRef]
16. Li, J.; Li, Z.; Gong, H.; Ma, M.; Li, S.; Yang, H.; Zhang, H.; Liu, J. Identification and characterization of a novel high-activity amylosucrase from *Salinispirillum* sp. LH10-3-1. *Appl. Microb. Biot.* **2023**, *107*, 1725–1736. [CrossRef]
17. Sedmak, J.J.; Grossberg, S.E. A rapid, sensitive and vertile assay for protein using Coomassia Brilliant Blue G250. *Anal. Biochem.* **1977**, *79*, 544–552. [CrossRef]
18. Zhong, W.; Yang, M.; Mu, T.; Wu, F.; Hao, X.; Chen, R.; Sharshar, M.M.; Thygesen, A.; Wang, Q.; Xing, J. Systematically redesigning and optimizing the expression of D-lactate dehydrogenase efficiently produces high-optical-purity D-lactic acid in *Saccharomyces cerevisiae*. *Biochem. Eng. J.* **2019**, *144*, 217–226. [CrossRef]
19. Sam, K.K.; Lau, N.S.; Furusawa, G.; Amirul, A.A. Draft genome sequence of halophilic *Hahella* sp. strain CCB-MM4, isolated from Matang Mangrove Forest in Perak, Malaysia. *Genome Announc.* **2017**, *5*, e01147-17. [CrossRef]
20. Liao, H.; Li, Y.Q.; Guo, X.T.; Lin, X.L.; Lai, Q.L.; Xu, H.; Zheng, T.L.; Tian, Y. *Mangrovitalea sediminis* gen. nov. sp. nov. a member of the family *Alteromonadaceae* isolated from mangrove sediment. *Int. J. Syst. Evol. Microbiol.* **2017**, *67*, 5172–5178. [CrossRef]
21. Christiansen, L.; Bech, P.K.; Schultz-Johansen, M.; Martens, H.J.; Stougaard, P. *Colwellia* echini sp. nov. an agar- and carrageenan-solubilizing bacterium isolated from sea urchin. *Int. J. Syst. Evol. Microbiol.* **2018**, *68*, 687–691. [CrossRef]
22. Liu, C.; Chen, C.X.; Zhang, X.Y.; Yu, Y.; Liu, A.; Li, G.W.; Chen, X.L.; Chen, B.; Zhou, B.C.; Zhang, Y.Z. *Marinobacter antarcticus* sp. nov. a halotolerant bacterium isolated from Antarctic intertidal sandy sediment. *Int. J. Syst. Evol. Microbiol.* **2012**, *62*, 1838–1844. [CrossRef]
23. Zaboli, M.; Saeidnia, F.; Zaboli, M.; Torkzadeh-Mahani, M. Stabilization of recombinant D-Lactate dehydrogenase enzyme with trehalose: Response surface methodology and molecular dynamics simulation study. *Process Biochem.* **2021**, *101*, 26–35. [CrossRef]
24. Kochhar, S.; Hunziker, P.E.; Leong-Morgenthaler, P.; Hottinger, H. Primary structure, physicochemical properties, and chemical modification of NAD^+-dependent D-lactate dehydrogenase. *J. Biol. Chem.* **1992**, *267*, 8499–8513. [CrossRef]
25. Taguchi, H.; Ohta, T. D-lactate dehydrogenase is a member of D-isomer-specific 2-hydroxy acid dehydrogenase family. Cloning, sequencing, and expression in Escherichia coli of the D-lactate dehydrogenase gene of *Lactobacillus plantarum*. *J. Biol. Chem.* **1991**, *266*, 12588–12594. [CrossRef]
26. Bhowmik, T.; Lueck, M.; Steele, J.L. Purification and partial characterization of D-(−)-lactate dehydrogenase from *Lactobacillus helveticus* CNRZ 32. *J. Indust. Microbiol.* **1993**, *12*, 35–41. [CrossRef]
27. Isobe, K.; Koide, Y.; Yokoe, M.; Wakao, N. Crystallization and some properties of D-lactate dehydrogenase from *Staphylococcus* sp. LDH-1. *J. Biosci. Bioeng.* **2002**, *94*, 330–335. [CrossRef]
28. Gulmez, C.; Altinkaynak, C.; Özdemir, N.; Atakisi, O. Proteinase K hybrid nanoflowers (P-hNFs) as a novel nanobiocatalytic detergent additive. *Int. J. Biol. Macromol.* **2018**, *119*, 803–810. [CrossRef]
29. Zhu, P.; Wang, Y.; Li, G.; Liu, K.; Liu, Y.; He, J.; Lei, J. Preparation and application of a chemically modified laccase and copper phosphate hybrid flower-like biocatalyst. *Biochem. Eng. J.* **2019**, *144*, 235–243. [CrossRef]

30. Bernard, N.; Ferain, T.; Garmyn, D.; Hols, P.; Delcour, J. Cloning of the D-lactate dehydrogenase gene from *Lactobacillus delbrueckii* subsp. *bulgaricus* by complementation in *Escherichia coli*. *FEBS Lett.* **1991**, *290*, 61–64.
31. Singh, S.K.; Ahmed, S.U.; Pandey, A. Metabolic engineering approaches for lactic acid production. *Process Biochem.* **2006**, *41*, 991–1000. [CrossRef]
32. Li, X.; Jiang, B.; Pan, B.; Mu, W.; Zhang, T. Purification and partial characterization of *Lactobacillus* species SK007 lactate dehydrogenase (LDH) catalyzing phenylpyruvic acid (PPA) conversion into phenyllactic acid (PLA). *J. Argric. Food Chem.* **2008**, *56*, 2392–2399. [CrossRef]
33. Zhou, X.; Zhou, J.; Xin, F.; Ma, J.; Zhang, W.; Wu, H.; Jiang, M.; Dong, W. Heterologous expression of a novel D-lactate dehydrogenase from *Lactobacillus* sp. ZX1 and its application for D-phenyllactic acid production. *Int. J. Biol. Macromol.* **2018**, *119*, 1171–1178. [CrossRef]
34. Kochhar, S.; Lamzin, V.S.; Razeto, A.; Delley, M.; Hottinger, H.; Germond, J.E. Roles of His205, His296, His303 and Asp259 in catalysis by NAD^+-specific D-lactate dehydrogenase. *Eur. J. Biochem.* **2000**, *267*, 1633–1639. [CrossRef]
35. Razeto, A.; Kochhar, S.; Hottinger, H.; Dauter, M.; Wilson, K.S.; Lamzin, V.S. Domain closure, substrate specificity and catalysis of D-lactate dehydrogenase from *Lactobacillus bulgaricus*. *J. Mol. Biol.* **2002**, *318*, 109–119. [CrossRef]
36. Satomura, T.; Kawakami, R.; Sakuraba, H.; Ohshima, T. A novel flavin adenine dincleotide (FAD) containing D-lactate dehydrogenase from the thermoacidophilic crenarchaeota *Sulfolobus tokodaii* strain 7: Purification, characterization and expression in *Escherichia coli*. *J. Biosci. Bioeng.* **2008**, *106*, 16–21. [CrossRef]
37. Garvie, E.I. Bacterial lacate dehydrogenases. *Microbiol. Rev.* **1980**, *44*, 106–139. [CrossRef]
38. Nakano, K.; Sawada, S.; Yamada, R.; Mimitsuka, T.; Ogino, H. Enhancement of the catalytic activity of D-lactate dehydrogenase from *Sporolactobacillus laevolacticus* by site-directed mutagenesis. *Biochem. Eng. J.* **2018**, *133*, 214–218. [CrossRef]
39. Li, J.; Li, Z.; Cao, M.; Liu, J. Expression and characterization of catechol 1,2-dioxygenase from *Oceanimonas marisflavi* 102-Na3. *Protein Expr. Purif.* **2021**, *188*, 105964. [CrossRef]
40. Taguchi, H.; Ohta, T. Involvement of Glu-264 and Arg-235 in the essential interaction between the catalytic imidazole and substrate for the D-lactate dehydrogenase catalysis. *J. Biochem.* **1997**, *122*, 802–809. [CrossRef]
41. Zhang, L.; Ma, Y.; Wang, C.; Wang, Z.; Chen, X.; Li, M.; Zhao, R.; Wang, L. Application of dual-enzyme nanoflower in the epoxidation of alkenes. *Process Biochem.* **2018**, *74*, 103–107. [CrossRef]
42. Somturk, B.; Yilmaz, I.; Altinkaynak, C.; Karatepe, A.; Özdemir, N.; Ocsoy, I. Synthesis of urease hybrid nanoflowers and their enhanced catalytic properties. *Enzym. Microb. Technol.* **2016**, *86*, 134–142. [CrossRef] [PubMed]